OH Reaction Kinetics of Polycyclic Aromatic Hydrocarbons and Polychlorinated Dibenzo-*p*-dioxins and Dibenzofurans

W. Wayne Brubaker, Jr., and Ronald A. Hites*

School of Public and Environmental Affairs and Department of Chemistry, Indiana University, Bloomington, Indiana 47405

Received: July 1, 1997; In Final Form: October 14, 1997

Rate constants were measured for gas-phase reactions of the hydroxyl radical (OH) with six polycyclic aromatic hydrocarbons (PAH) and four polychlorinated dibenzo-*p*-dioxins and dibenzofurans (PCDD/F). These OH reaction rate constants were determined in helium at about 1 atm over various temperature ranges between 306 and 405 K. The experiments were carried out in a small, heated quartz reaction chamber sampled by on-line mass spectrometry, and OH was produced by the photolysis of O_3 in the presence of H_2O. Arrhenius regressions were performed with the rate constants of each compound, and the temperature dependencies were found to be slight to nonexistent. The OH reaction rate constants of PCDD/F were in agreement with those predicted by a structure−reactivity method. The resulting rate constants at 298 K (in units of 10^{-12} cm^3 s^{-1}) were as follows: naphthalene, 23; acenaphthene, 58; fluorene, 13; phenanthrene, 27; anthracene, 190; fluoranthene, 11; dibenzo-*p*-dioxin, 12; 2,7-dichlorodibenzo-*p*-dioxin, 4.4; dibenzofuran, 3.5; and 2,8-dichlorodibenzofuran, 2.2.

Introduction

Polycyclic aromatic hydrocarbons (PAH) and polychlorinated dibenzo-*p*-dioxins and dibenzofurans (PCDD/F) are emitted into the atmosphere from combustion sources and transported great distances before deposition to water or soil. PAH and PCDD/F are potentially harmful to humans,[1,2] and a knowledge of their atmospheric residence times and transformations is important. Atmospheric 2−4-ring PAH exist primarily in the gas phase, and OH reactions are expected to be a significant removal pathway.[1,3,4] Likewise, atmospheric PCDD/F with <5 chlorines exist largely in the gas phase,[5,6] and OH reactions will also be significant.[7] Thus, to assess the atmospheric behavior of these compounds, it is critical to know the rate constants for their gas-phase reactions with the hydroxyl radical (OH).

Experimental OH reaction rate constants exist in the literature for a number of PAH at about 300 K;[1,8] however, our laboratory recently developed a system for measuring OH reaction rate constants for gas-phase, semivolatile organic compounds, such as PAH as a function of temperature.[9] Unlike traditional reaction systems, our system allows rate constant measurements at above ambient temperatures; these rate constants can then be extrapolated to environmentally significant temperatures by use of the Arrhenius equation. A better knowledge of the temperature dependence of PAH−OH reactions would be useful for atmospheric modeling, given that the temperature of the troposphere ranges from 190 to 305 K, depending on latitude and altitude.[10] Only naphthalene, biphenyl, and phenanthrene have been studied over a range of temperatures.[8,11] In this paper, we present OH reaction rate constant measurements and related temperature-dependent parameters for six PAH over various temperature ranges between 306 and 386 K. These results include the first OH reaction rate constant measurements for a 4-ring PAH, fluoranthene.

For PCDD/F, experimental OH reaction rate constants only had been measured for dibenzo-*p*-dioxin, dibenzofuran,[12] and 1-chlorodibenzo-*p*-dioxin[13] at about 300 K. A recent modification to our system allowed us to measure OH reaction constants for 1,2,3,4-tetrachlorodibenzo-*p*-dioxin over the temperature range 373−405 K but did not allow similar measurements for PCDD/F above or below a chlorination level of four.[14] Returning to our initial system,[9,11] OH reaction rate constants are now presented for dibenzo-*p*-dioxin and dibenzofuran and a dichlorinated dioxin and furan over temperature ranges between 345 and 405 K. Arrhenius extrapolations of these rate constants and their agreement with rate constants predicted by a structure−reactivity method[7] are discussed.

Experimental Section

OH reaction rate experiments were carried out in a reaction system similar to one described in detail elsewhere.[9,11,14] The present system consists of a 160 mL quartz reaction chamber that is mounted in the oven of a gas chromatograph (for temperature control) and sampled by on-line mass spectrometry. Helium (99.999%; Gas Tech, Hillside, IL) served as the diluent gas for all experiments, and the pressure inside the chamber was held at approximately 1 atm. OH radicals were produced in situ by

$$O_3 + h\nu\ (\lambda \leq 315\ \text{nm}) \rightarrow O(^1D) + O_2 \qquad (1)$$

$$O(^1D) + H_2O \rightarrow 2OH \qquad (2)$$

O_3 was produced by flowing O_2 (99.998% purity; Air Products, Allentown, PA) through a 12 kV discharge prior to chamber introduction. Water vapor was introduced by bubbling the He gas flow through H_2O (HPLC grade; EM Science, Gibbstown, NJ) at about 295 K. The He/H_2O to O_2/O_3 ratio of the total diluent gas was approximately 100−500, and O_3 concentrations ranged between approximately 0.9×10^{15} and 9×10^{15} cm^{-3} within the chamber at about 300 K. UV radiation centered at

S1089-5639(97)02119-1 CCC: $15.00
Published on Web 01/22/1998

TABLE 1: Compounds Studied with Their Monitored Ions

compound	ions monitored (m/z)	source of ion[a]
naphthalene	128	M^+
acenaphthene[b]	154	M^+
fluorene	166	M^+
phenanthrene	178	M^+
anthracene	178	M^+
fluoranthene	202	M^+
dibenzo-*p*-dioxin	184	M^+
dibenzofuran	168	M^+
2,7-dichlorodibenzo-*p*-dioxin	252	M^+
2,8-dichlorodibenzofuran	236	M^+
cyclohexane[c]	56	$(M-C_2H_4)^+$
2-propanol[c]	45	$(M\text{-}CH_3)^+$
toluene[c]	91	$(M-H)^+$

[a] M = molecular ion. [b] Both a test compound and a reference compound in this study. [c] Reference compound used with relative rate technique.

254 nm was provided by a mercury, Pen-Ray lamp (UVP, Upland, CA).

OH reaction rate constants were measured by the widely accepted relative rate technique.[8,15] The reference compounds used in this study were cyclohexane (Aldrich, Milwaukee, WI), 2-propanol, and toluene (EM Science). The PAH we studied are listed in Table 1; they were acquired from Aldrich, with the exception of fluorene and phenanthrene (Eastman, Rochester, NY). Note that acenaphthene served as a reference compound in experiments with anthracene, using our experimental results for acenaphthene relative to both cyclohexane and toluene. The unsubstituted and chlorinated dioxins and furans (see Table 1) were from AccuStandard (New Haven, CT). Approximately 2−20 μg each of a reference compound and a test compound, both dissolved in CCl_4 (Aldrich), were injected into the closed reaction chamber for each experiment. PAH and PCDD/F concentrations were approximately $(0.7-6) \times 10^{14}$ cm^{-3}, and those for the reference compounds were approximately $(2-4) \times 10^{14}$ cm^{-3}. The reactants were monitored by on-line, electron-impact mass spectrometry (EI-MS), using a Hewlett-Packard 5985B mass spectrometer in its selected ion monitoring (SIM) mode. The m/z values selected to monitor each compound are given in Table 1 and represent, in most cases, the compounds' molecular ions.

The reaction chamber was irradiated 1−3 times during each experiment for durations of 1−5 min each. Assuming OH reactions were the primary loss processes during UV irradiation of the chamber, the recorded signal intensities for the two compounds follow the equation

$$\ln \frac{[\text{test}]_0}{[\text{test}]_t} = \left(\frac{k_{\text{test}}}{k_{\text{ref}}}\right) \ln \frac{[\text{reference}]_0}{[\text{reference}]_t} \qquad (3)$$

where the signal intensities were measured at time $t = 0$ and at subsequent times t. The values k_{test} and k_{ref} represent the OH reaction rate constants for the test and reference compounds, respectively. Values of k_{test} were calculated from the slopes of experimental plots of eq 3 and the temperature-dependent expressions of k_{ref} most recently recommended by Atkinson.[8,16] Other potential loss processes of the reactants that could interfere with our OH rate constant measurements, such as dark reactions with ozone or losses to the chamber walls, were accounted for by analysis of the signal intensities before and after the UV irradiation.

Results and Discussion

PAH[17] and PCDD/F[7] absorb mid-UV radiation; however, direct photolysis during our experiments was negligible because the radiation flux of the lamp (approximately 300 mW/cm^2) was low. This was confirmed by control experiments under typical experimental conditions where O_3, the OH precursor, was not introduced. Each compound was separately introduced into the reaction chamber which was held at 100 °C with a He:O_2 ratio of approximately 100:1. In each experiment, the signal monitored for the analyte did not change when the UV lamp was turned on for 5 min and then turned off.

Since the conditions were similar to those of previous studies using this system,[9,11,14] we expected no interference of $O(^1D)$, $O(^3P)$, or $O(^1D)-CCl_4$ reaction products in our OH reaction rate measurements. We also note that toluene−OH reaction rate constants previously measured with this reaction system by Anderson and Hites did not depend on the O_2 concentration, which was varied between 0.4% and 95%.[9] Therefore, we anticipated no effects caused by varying O_2 concentrations here.

Heterogeneous reactions on the chamber's walls, known as "wall effects", were expected to be insignificant in our experiments. Wall effects in OH reaction studies are typically associated with NO_X chemistry, which is linked to the photolysis of alkyl nitrites and the use of NO in air for OH production. Our OH production scheme did not involve NO_X, nor did we use air or N_2 as a diluent gas. More importantly, our mass spectrometer monitors reactants via a capillary positioned in the middle of the reaction chamber. This capillary samples at an approximate rate of 0.4 mL/min; therefore, the maximum volume sampled for a 5 min irradiation is only about 2 mL. Since this volume is taken from the center of the chamber and only represents approximately 1% of the total volume, any possible wall effects would be minimized.

The results for our PAH−OH and PCDD/F−OH experiments are given in Table 2. The average 95% confidence limit for the rate constant ratios, $k_{\text{test}}/k_{\text{ref}}$, was approximately 2%. Given the difficulty of some of these measurements, the uncertainty in the $k_{\text{test}}/k_{\text{ref}}$ values for the less volatile compounds could be more than 2% due to the increased importance of background subtraction and greater subjectivity in accounting for the pre- and post-UV signal trends. The background subtraction is only significant for the least volatile of the analytes, such as 2,7-dibenzo-*p*-dioxin, where we estimated the maximum uncertainty due to background subtraction to be 25%. The largest value of relative standard deviation (RSD) for any compound's measurements at any particular temperature is approximately 15%, which should reflect any discrepancies due to analysis and subtraction of non-UV decay. However, the uncertainties stated for our final rate constants reflect the published uncertainties for the reference rate constants (25−35%), and these certainly exceed any uncertainty attributed to our data analysis. The natural logarithms of the rate constants for each compound in Table 2 were fitted by a linear regression to the reciprocal of the experimental temperature. These regressions are summarized in Table 3 where the Arrhenius parameters (preexponential factor and activation energy, E_a) are listed.

PAH−OH Reactions. The primary route of reaction for any PAH is expected to be OH attack of an aromatic ring:[1,8,18]

$$\text{OH} + \text{PAH} \rightarrow \text{OH-PAH}^* \qquad (4)$$

where the energetic, OH−PAH* adduct can become collision-

TABLE 2: Experimental Rate Constant Ratios and Rate Constants for PAH−OH and PCDD/F−OH Reactions

T (K)	k_{test}/k_{ref}[a]	rate const ($\times 10^{-12}$ cm^3 s^{-1})[b]	T (K)	k_{test}/k_{ref}[a]	rate const ($\times 10^{-12}$ cm^3 s^{-1})[b]	T (K)	k_{test}/k_{ref}[a]	rate const ($\times 10^{-12}$ cm^3 s^{-1})[b]
				Naphthalene				
306	2.99 ± 0.04	23 ± 6	336	2.68 ± 0.01	22 ± 6	306	4.35 ± 0.18[c]	23 ± 8[c]
306	2.85 ± 0.05	22 ± 5	366	2.60 ± 0.03	24 ± 6	336	4.98 ± 0.01[c]	27 ± 9[c]
307	3.01 ± 0.02	23 ± 6	366	2.50 ± 0.04	23 ± 6	366	4.34 ± 0.02[c]	24 ± 8[c]
336	2.66 ± 0.01	22 ± 6	306	4.76 ± 0.06[c]	25 ± 9[c]	366	4.23 ± 0.09[c]	23 ± 8[c]
				Acenaphthene				
325	7.6 ± 0.3	62 ± 15	346	7.1 ± 0.2	61 ± 15	325	11.1 ± 1.2[d]	60 ± 15[d]
325	7.7 ± 0.2	63 ± 16	365	6.80 ± 0.07	62 ± 15	345	11.6 ± 0.2[d]	59 ± 15[d]
345	7.2 ± 0.2	61 ± 15	366	7.72 ± 0.07	70 ± 18	365	12.8 ± 0.2[d]	61 ± 15[d]
				Fluorene				
326	1.73 ± 0.03	14 ± 3	346	1.63 ± 0.01	14 ± 4	366	1.55 ± 0.01	14 ± 4
326	1.71 ± 0.03	14 ± 3	346	1.60 ± 0.01	14 ± 3	366	1.58 ± 0.01	14 ± 4
326	1.54 ± 0.02	13 ± 3						
				Dibenzofuran				
345	0.49 ± 0.01	4.2 ± 1.0	366	0.53 ± 0.01	4.8 ± 1.2	385	0.51 ± 0.01	5.0 ± 1.2
345	0.51 ± 0.01	4.4 ± 1.1	366	0.56 ± 0.01	5.1 ± 1.3	386	0.58 ± 0.01	5.6 ± 1.4
345	0.56 ± 0.01	4.8 ± 1.2	366	0.53 ± 0.01	4.8 ± 1.2	386	0.54 ± 0.01	5.2 ± 1.3
345	0.57 ± 0.01	4.9 ± 1.2	366	0.54 ± 0.01	4.9 ± 1.2	386	0.60 ± 0.01	5.8 ± 1.5
				Dibenzo-*p*-dioxin				
345	1.42 ± 0.01	12 ± 3	365	1.28 ± 0.01	12 ± 3	385	1.22 ± 0.01	12 ± 3
345	1.42 ± 0.01	12 ± 3	365	1.30 ± 0.01	12 ± 3	385	1.30 ± 0.01	13 ± 3
345	1.42 ± 0.01	12 ± 3	365	1.36 ± 0.01	12 ± 3	385	1.25 ± 0.01	12 ± 3
345	1.46 ± 0.01	13 ± 3	365	1.36 ± 0.01	12 ± 3	385	1.28 ± 0.01	12 ± 3
				Phenanthrene				
346	2.89 ± 0.06	25 ± 6	366	2.79 ± 0.04	25 ± 6	384	2.56 ± 0.02	25 ± 6
346	3.1 ± 0.1	26 ± 7	366	2.56 ± 0.02	23 ± 6	385	2.63 ± 0.02	25 ± 6
346	2.85 ± 0.09	25 ± 6	375	2.81 ± 0.02	26 ± 7	385	2.14 ± 0.04	21 ± 5
365	2.59 ± 0.06	24 ± 6	375	2.73 ± 0.03	26 ± 6	386	2.58 ± 0.02	25 ± 6
366	2.37 ± 0.02	22 ± 5	375	2.55 ± 0.03	24 ± 6	386	2.20 ± 0.04	21 ± 5
365	2.56 ± 0.04	23 ± 6	376	2.58 ± 0.04	24 ± 6			
366	2.44 ± 0.02	22 ± 6	376	2.55 ± 0.03	24 ± 6			
				Anthracene				
346	2.61 ± 0.07[e]	160 ± 40[e]	346	2.90 ± 0.05[e]	180 ± 50[e]	365	2.48 ± 0.08[e]	160 ± 40[e]
346	2.7 ± 0.1[e]	170 ± 40[e]	346	2.87 ± 0.08[e]	180 ± 40[e]	365	2.69 ± 0.08[e]	170 ± 40[e]
346	3.39 ± 0.06[e]	210 ± 50[e]	365	2.95 ± 0.07[e]	190 ± 50[e]	365	3.0 ± 0.2[e]	190 ± 50[e]
346	3.15 ± 0.05[e]	200 ± 50[e]	365	3.05 ± 0.07[e]	190 ± 50[e]			
				2,8-Dichlorodibenzofuran				
355	0.34 ± 0.01	3.0 ± 0.7	376	0.39 ± 0.01	3.7 ± 0.9	395	0.39 ± 0.01	3.9 ± 1.0
355	0.35 ± 0.01	3.1 ± 0.8	376	0.38 ± 0.01	3.5 ± 0.9	395	0.37 ± 0.01	3.7 ± 0.9
355	0.32 ± 0.01	2.8 ± 0.7	376	0.39 ± 0.01	3.7 ± 0.9	395	0.35 ± 0.01	3.5 ± 0.9
365	0.36 ± 0.01	3.3 ± 0.8	376	0.39 ± 0.01	3.6 ± 0.9	395	0.33 ± 0.01	3.3 ± 0.8
365	0.35 ± 0.01	3.2 ± 0.8	376	0.39 ± 0.01	3.7 ± 0.9	405	0.38 ± 0.01	3.9 ± 1.0
365	0.37 ± 0.01	3.3 ± 0.8	376	0.39 ± 0.01	3.7 ± 0.9	405	0.39 ± 0.01	4.0 ± 1.0
365	0.36 ± 0.01	3.2 ± 0.8	395	0.37 ± 0.01	3.7 ± 0.9			
				2,7-Dichlorodibenzo-*p*-dioxin				
355	0.77 ± 0.04	6.8 ± 1.7	375	0.74 ± 0.01	7.0 ± 1.7	395	0.93 ± 0.01	9.2 ± 2.3
365	0.83 ± 0.02	7.5 ± 1.9	375	0.83 ± 0.01	7.7 ± 1.9	395	0.83 ± 0.01	8.3 ± 2.1
365	0.85 ± 0.02	7.8 ± 1.9	375	0.85 ± 0.01	7.9 ± 2.0	395	0.86 ± 0.02	8.5 ± 2.1
365	0.75 ± 0.01	6.9 ± 1.7	375	0.82 ± 0.01	7.7 ± 1.9			
				Fluoranthene				
356	1.98 ± 0.05	18 ± 4	386	2.59 ± 0.03	25 ± 6	386	4.1 ± 0.2[c]	22 ± 8[c]
366	1.94 ± 0.05	18 ± 4	376	3.48 ± 0.04[c]	19 ± 7[c]	356	3.85 ± 0.07[d]	19 ± 5[d]
366	2.20 ± 0.03	20 ± 5	376	2.96 ± 0.04[c]	16 ± 6[c]	366	4.02 ± 0.08[d]	19 ± 5[d]
376	2.19 ± 0.07	21 ± 5	386	3.69 ± 0.05[c]	20 ± 7[c]			

[a] Reference compound was cyclohexane, unless otherwise noted. Stated uncertainties of the rate constant ratios represent 95% confidence limits. [b] Stated uncertainties of the experimental rate constants reflect the estimated overall uncertainty recommended for the reference rate constants: cyclohexane, ±25%;[8] 2-propanol, ±35%;[16] toluene, ±25%;[8] and acenaphthene, ±25% (this study). [c] Reference compound was 2-propanol. [d] Reference compound was toluene. [e] Reference compound was acenaphthene, using our experimentally derived Arrhenius expression for acenaphthene.

ally stabilized by the surrounding gas (M):

$$\text{OH}-\text{PAH}^* \xrightarrow{\text{M}} \text{OH}-\text{PAH} \qquad (5)$$

Under atmospheric conditions, it can then react with oxygen and form products:

$$\text{OH}-\text{PAH} + \text{O}_2 \rightarrow \text{products} \qquad (6)$$

For all but one of the PAH, the activation energies were essentially zero (see Table 3), and this suggests that these PAH proceed through reactions 4 and 5. Greater, but still slight, temperature dependencies were expected based on the previous data of Lorenz and Zellner and on the expressions recommended by Atkinson for naphthalene and phenanthrene (see Figures 1 and 2, respectively), where the activation energies were negative.[8,19] A negative temperature dependence for a PAH indicates that the reverse of reaction 4 becomes more rapid at higher temperatures. Note, however, that the disagreement between our data and that of Lorenz and Zellner could be due to differences in experimental pressures: approximately 1 atm for

TABLE 3: Temperature Dependence of Experimentally Determined OH Reaction Rate Constants

compound	no. of expts	preexponential factor ($\times 10^{-12}$ cm^3 s^{-1})	E_a (kJ/mol)[a]
naphthalene	12	24	0.04 ± 0.59
acenaphthene	9	93	1.2 ± 1.0
fluorene	7	23	1.4 ± 0.9
phenanthrene	19	14	-1.6 ± 1.4
anthracene	11	130	-0.9 ± 3.0
fluoranthene	11	210	7.3 ± 3.3
dibenzo-*p*-dioxin	12	11	-0.29 ± 0.49
dibenzofuran	12	22	4.6 ± 1.1
2,7-dichlorodibenzo-*p*-dioxin	11	66	6.7 ± 1.5
2,8-dichlorodibenzofuran	20	21	5.6 ± 0.9

[a] Uncertainty in E_a is based on one standard error of the slope of the temperature dependence regression.

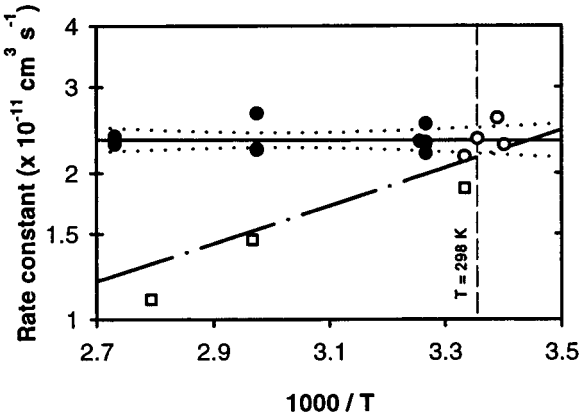

Figure 1. Arrhenius plot for naphthalene−OH reaction. Symbols: ●, this study; ○, approximately 300 K rate constants of four separate studies;[8] □, data from Lorenz and Zellner.[8,19] Lines: solid, fit to our data; dotted, 95% confidence limits of our fit; dashed, Atkinson's recommendation.[8]

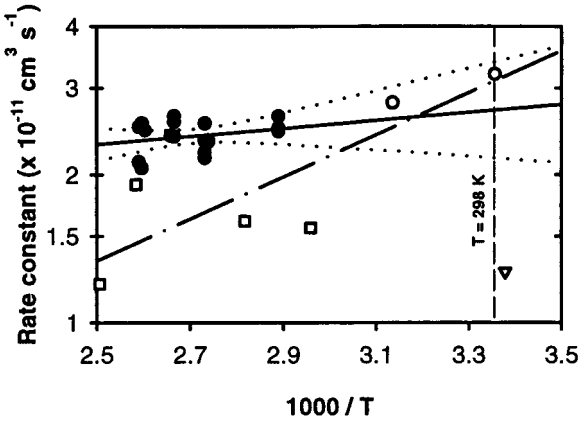

Figure 2. Arrhenius plot for phenanthrene−OH reaction. Symbols: ●, this study; ○, data from Biermann et al.;[25] □, data from Lorenz and Zellner;[8] ▽, data from Kwok et al.[26] Lines: solid, fit to our data; dotted, 95% confidence limits of our fit; dashed, Atkinson's recommendation.[8]

our system versus an approximate maximum of 1.3×10^{-3} atm for their laser photolysis system.[19] Despite the disagreement at above ambient temperatures, the Arrhenius extrapolation of our experimental naphthalene−OH reaction rate constants agreed with 298 K measurements made by other groups (see Figure 1 and Table 4).

An Arrhenius plot for our acenaphthene−OH reaction rate constants is shown in Figure 3. Acenaphthene was used in our anthracene−OH experiments as the reference compound since it was the "fastest" OH-reacting compound we had available.

TABLE 4: Experimental and Calculated PAH−OH Reaction Rate Constants at 298 K

compound	exptl k^{298K} from this study ($\times 10^{-12}$ cm^3 s^{-1})[a]	lit. rate const at RT ($\times 10^{-12}$ cm^3 s^{-1})[a]	ref
naphthalene	23 (22−25)	21.6 (15.1−28.1)[b]	8
acenaphthene	58 (52−66)	58.4	20
		103 (90−116)	21
fluorene	13 (11−15)	13.0	20
		16 (11−21)	24
phenanthrene	27 (22−34)	31 (19−43)	8
		12.7 (10.4−15.0)	26
anthracene	190 (120−290)	110 (101−119)[c]	25
		13 (6−20)	26
		17 (11−23)	24
fluoranthene	11 (6−19)		

[a] Values in parentheses represent stated ranges of uncertainty. Those for our experimental data represent 95% confidence limits of the temperature dependence regression. [b] Value recommended from the results of five studies. [c] Measurement made at 325 K.

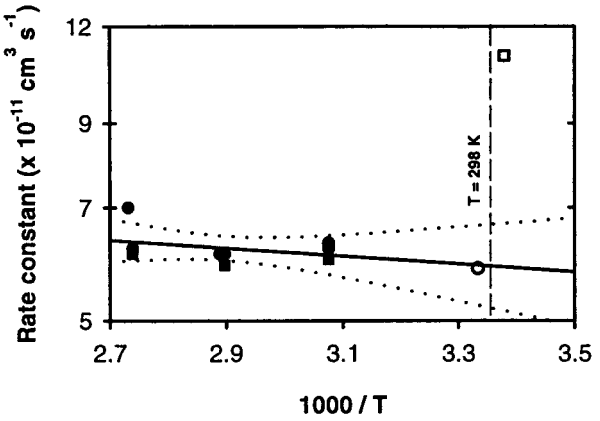

Figure 3. Arrhenius plot for acenaphthene-OH reaction. Symbols: ●, this study where cyclohexane was the reference; ■, this study where toluene was the reference; ○, data from Klopffer et al.;[20] □, data from Atkinson and Aschmann.[21] Lines: solid, fit to our data; dotted, 95% confidence limits of our fit.

This strategy was required to make our relative rate measurements of the even faster anthracene−OH reactions (discussed below). Note that the two sets of acenaphthene−OH rate constants, obtained using two different reference compounds, agree. Figure 3 and Table 4 also show that our acenaphthene−OH reaction rate constant estimated for 298 K agreed with that of Klopffer et al.[20] but differed from that of Atkinson and Aschmann by nearly a factor of 2.[21] Klopffer et al. later noted that their rate constant may be less reliable.[22] Klamt estimated an acenaphthene−OH reaction rate constant of 80×10^{-12} cm^3 s^{-1},[23] and this value, based on molecular orbital calculations, falls between our value and that of Atkinson and Aschmann.[21] Our extrapolation for fluorene (see Table 4) agreed with both the measurements of Klopffer et al.[20] and of Kwok et al.[24]

Our OH reaction rate constant measurements for phenanthrene and anthracene require further discussion. The extrapolation of our phenanthrene data (see Figure 2 and Table 4) agreed with the extrapolation by Atkinson[8] from data obtained by Biermann et al.[25] and Lorenz and Zellner. In a later study, Kwok et al. suggested that the study of Biermann et al. was erroneous and that the rate constant is essentially independent of temperature and should have a value of $(15 \pm 6) \times 10^{-12}$ cm^3 s^{-1}.[26] In which case, our estimated rate constant at 298 K (see Table 4) is high by a factor of about 2. There also appears to be discrepancies between our data and measurements available in the literature for anthracene (see Table 4). Our estimated

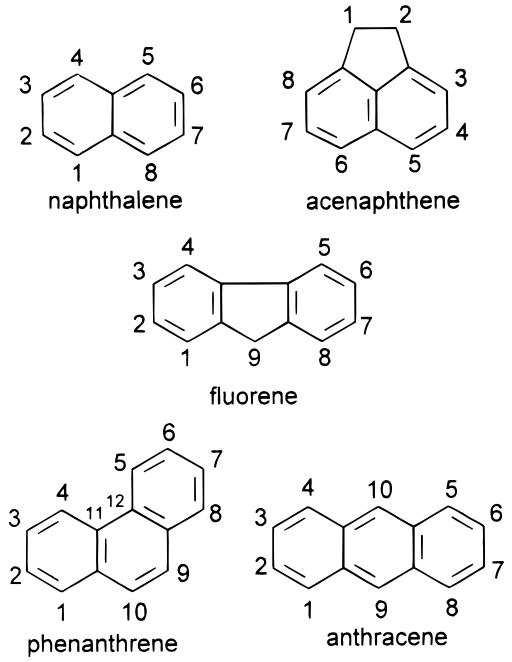

Figure 4. Structures of PAH discussed in the text.

rate constant at 298 K for its OH reaction was higher than that of Biermann et al. at 325 K by a factor of about 2.[25] Kwok et al. recently reported rate constants at 296−297 K, which are lower than our value by at least an order of magnitude.[24,26] It is interesting to note that our value is in excellent agreement with the value of 200×10^{-12} cm^3 s^{-1} predicted by Klamt from molecular orbital calculations of anthracene.[23]

No OH reaction rate constants have been reported in the literature for fluoranthene. An Arrhenius regression, significant at the 95% confidence level, gave a positive, yet small, E_a value for fluoranthene (see Table 3). This positive activation energy indicates that fluoranthene's OH−PAH* adduct is less likely to thermally decompose back to reactants (the reverse of reaction 4) at higher temperatures. Note fluoranthene was the only 4-ring PAH studied, and its OH−PAH* adduct is probably more stable than those of the other PAH presented here.

We should note that phenanthrene, anthracene, and fluoranthene were much more difficult to work with experimentally, relative to the other PAH. In general, the presence of O_3 reduced our experimental sensitivity and significantly increased the observed dark decay of PAH in the reaction chamber. These undesirable effects were more problematic with phenanthrene, anthracene, and fluoranthene due to their lower vapor pressures and, perhaps, greater reactivities with O_3.[1,24,26] Non-UV decays, for all PAH in the presence of O_3, were more pronounced at the higher experimental temperatures which were sometimes necessary to detect these less volatile PAH. The O_3 concentrations had to be reduced for experiments with anthracene and fluoranthene relative to those for the other PAH. Still, the dark decay could account for up to 60% of the total decay observed while the UV lamp was on during a typical fluoranthene experiment. While these problems with O_3 might explain the scatter in our measured phenanthrene−OH and anthracene−OH reaction rate constants (for example, see Figure 2), we still have no explanation for the systematic differences between our data and measurements in the literature for these two PAH, especially anthracene.

A comparison of the individual PAH structures (see Figure 4) gives some insight about the differences among their OH reaction rate constants. Naphthalene and acenaphthene both consist of two fused aromatic rings, but acenaphthene's OH reaction rate is possibly enhanced (see Table 4) by significant H atom abstraction, which is likely to occur at the saturated two-carbon moiety forming a fused cyclopentyl ring.[1,21] Such a comparison among the 3-ring PAH is not as easy, given the discrepancies between our data and those in the literature. The recent work of Kwok et al. gave OH reaction rate constants for fluorene, phenanthrene, and anthracene, which were essentially the same for all three compounds.[24,26] However, our results and those of Biermann et al.[25] clearly demonstrated anthracene to be much more reactive than the other two compounds (see Table 4). OH reaction product studies of fluorene and phenanthrene[27,28] indicate OH radical attack most likely occurs at the 9-position for all three of these compounds (see Figure 4). The difference between the reaction rates of fluorene and anthracene could be explained by the different reaction pathways available at their 9-positions. Fluorene can undergo H atom abstraction at the 9-position to form fluorenone, while anthracene requires OH attack on the aromatic ring.

This reasoning, however, does not explain the difference between phenanthrene and anthracene, which only differ structurally by the relative positions of their aromatic rings. Semiempirical molecular orbital calculations may provide some insight. The net atomic charge for each carbon in phenanthrene and anthracene has been calculated,[29] and those carbons with the most positive net charges were considered to be the most reactive positions. For example, anthracene's carbons at its 9-position and its identical 10-position have the most positive net charges relative to the other carbons on the molecule. However, for phenanthrene, the carbons with the most positive net charges were those at the 11- and 12-positions. Gas-phase reaction product studies clearly show the 9- and 10- positions of phenanthrene are the most reactive[26,28] and suggest that reactions at the 11- and 12-positions are stericly unfavorable given their locations inside the "bend" of the phenanthrene molecule (see Figure 4). Therefore, phenanthrene may not react with OH as efficiently as anthracene, a molecule in which the carbons with the most positive charges are stericly unhindered. This may explain the large differences we measured in the OH reaction rate constants for these two compounds.

PCDD/F−OH Reactions. Three of the four PCDD/F−OH reactions investigated here demonstrated a temperature dependence, which was significant at the 99% confidence level (see Table 3); dibenzo-*p*-dioxin's OH reaction rate was independent of temperature. Unlike the PAH−OH experiments discussed above, the presence of O_3 did not complicate our PCDD/F−OH experiments.

Ambient temperature PCDD/F−OH reaction rate constants were estimated for 298 K by Arrhenius extrapolations of our rate constants (see Table 5). Our rate constants for dibenzofuran and dibenzo-*p*-dioxin at 298 K agree well with those measured by Kwok et al.[12] In Table 5, we have also included similar experimental values from other PCDD/F studies in order to assess the method developed by Atkinson to predict PCDD/F−OH reaction rate constants.[7] The lower vapor pressures of PCDD/F, which range from 10^{-5} to 10^{-11} atm at 298 K,[30] make these compounds very difficult to study in traditional reaction systems held at room temperature. Therefore, the validity of Atkinson's structure−reactivity method is particularly important for modeling the atmospheric fates of PCDD/F. Our previous investigation of 1,2,3,4-tetrachlorodibenzo-*p*-dioxin found that its OH reaction rate constant at 298 K was in excellent agreement with that predicted by Atkinson.[14] While this value for 1,2,3,4-tetrachlorodibenzo-*p*-dioxin is a good indicator of

TABLE 5: Comparison of Experimental and Predicted PCDD/F−OH Reaction Rate Constants at 298 K

compound	exptl rate const ($\times 10^{-12}$ cm^3 s^{-1})[a]	ref	predicted rate const ($\times 10^{-12}$ cm^3 s^{-1})[b]
dibenzo-*p*-dioxin	12 (11−14)	this study	9.8
	14.8 (11.3−18.3)	12	
1-chlorodibenzo-*p*-dioxin	4.7 (3.1−6.3)	13	6.4
2,7-dichlorodibenzo-*p*-dioxin	4.4 (3.4−5.8)	this study	4.1
1,2,3,4-tetrachloro-dibenzo-*p*-dioxin	0.85 (0.47−1.6)	14	0.8
dibenzofuran	3.5 (2.9−4.2)	this study	7.0
	3.9 (3.0−4.8)	12	
2,8-dichlorodibenzo-furan	2.2 (1.8−2.5)	this study	2.5

[a] Values in parentheses represent stated ranges of uncertainty. Those for our experimental data represent 95% confidence limits of an Arrhenius regression of the temperature dependence regression. [b] Reference 7.

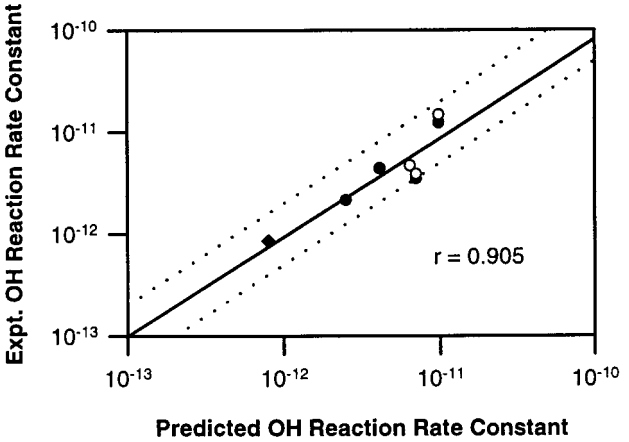

Figure 5. Comparison of experimental OH reaction rate constants and predicted OH reaction rate constants for PCDD/F.[7] Symbols: ●, this study; ◆, our previous study with 1,2,3,4-tetrachlorodibenzo-*p*-dioxin;[14] ○, values of Kwok et al. for dibenzo-*p*-dioxin, dibenzofuran,[12] and 1-chlorodibenzo-*p*-dioxin.[13] Lines: solid, fit to all experimental data and the predicted values; dotted, representation of disagreement with predicted values by a factor of 2.

the validity of the dioxin−OH rate constant predictions, not until now has experimental data been presented as a similar indicator for the furan−OH predictions. Our rate constant for 2,8-dichlorodibenzofuran agrees with that predicted by Atkinson's method (see last column of Table 5), thus validating this estimation technique for furan−OH reactions. In fact, all of the available experimental rate constants listed in Table 5 are within a factor of 2 of their predicted rate constants, and a regression between the logarithms of both values is significant at the 99.9% confidence level (see Figure 5). Therefore, Atkinson's OH reaction rate constant predictions are likely reliable for all 210 PCDD/F isomers.

Comparing the two compound classes (assuming equal degrees of chlorination), the experimental rate constants for the dioxins are higher than those for the furans, just as predicted. This further validates Atkinson's approach of treating each PCDD/F as two separate aromatic rings, each having two *ortho*-positioned substituents.[7] Considering unsubstituted PCDD/F as examples, the substituents would be two $-OC_6H_5$ groups for dibenzo-*p*-dioxin and a combination of $-OC_6H_5$ with $-C_6H_5$ for dibenzofuran. Given that $-OC_6H_5$ is less electrophilic than $-C_6H_5$, the substituent combination for the dioxin would mean its aromatic rings would be more likely to have an available electron, relative to the rings of the furan. This would make dibenzo-*p*-dioxin more susceptible to OH attack than dibenzofuran. Similarly, the same can be said of the observed rate constant trends based on chlorination levels within each class. As one increases the number of chlorines on a PCDD/F, the likelihood of an available electron on either aromatic ring decreases; thus, the OH reaction rate constants decrease as chlorination increases.

TABLE 6: Atmospheric Lifetimes Based on Gas-Phase OH Reactions

compound	atm lifetimes (h)[a]
naphthalene	12
acenaphthene	4.9
fluorene	22
phenanthrene	11
anthracene	1.5
fluoranthene	26
dibenzo-*p*-dioxin	24
dibenzofuran	82
2,7-dichlorodibenzo-*p*-dioxin	65
2,8-dichlorodibenzofuran	130

[a] Calculated using 9.7×10^5 cm^{-3} as the global OH concentration averaged over 24 h.[31]

Atmospheric Implications. Of the 10 PAH−OH and PCDD/F−OH reactions we studied, only those of fluoranthene, dibenzofuran, 2,8-dichlorodibenzofuran, and 2,7-dichlorodibenzo-*p*-dioxin were temperature-dependent. However, these temperature dependencies were found to be slight and could be considered insignificant from an environmental point of view. We estimated the OH reaction rate constants for these four compounds at 288 K, the average temperature of the earth's atmosphere, and found these values to be lower than those estimated at 298 K by an average of only 8%. This is less than the uncertainties for these values, and the 298 K rate constants reported here and elsewhere can be considered temperature independent for most atmospheric modeling purposes.

Gas-phase OH reactions are probably the most important atmospheric removal pathway for PAH and PCDD/F. The atmospheric lifetimes (τ) of these compounds can be approximated by

$$\tau = 1/k_{OH}[OH] \qquad (7)$$

where k_{OH} is a compound's second-order OH reaction rate constant and [OH] is the global OH concentration in the atmosphere, averaged over 24 h. Using our estimated OH reaction rate constants for 298 K (given in Tables 4 and 5) and [OH] $= 9.7 \times 10^5$ cm^{-3},[31] values of τ were calculated (see Table 6). In general, the atmospheric lifetimes of the PAH are less than a day, and those for the PCDD/F are greater than a day. Therefore, gas-phase PCDD/F, relative to PAH, are more likely to undergo atmospheric transport, to areas far removed from their sources. Note, however, that such approximations of τ are not valid for all PAH and PCDD/F. For example, acenaphthylene is much more reactive toward O_3 than most other PAH, and its atmospheric lifetime is predominantly controlled by gas-phase O_3 reactions.[1,21] Also, as the molecular weight and the chlorination levels of PAH and PCDD/F increase, larger fractions of these compounds are found in the atmosphere bound to particles, rather than remaining in the gas phase.[1,2,7,14] Therefore, the atmospheric removal of these higher molecular weight compounds is controlled to some degree by physical processes, such as wet and dry deposition.

Acknowledgment. The U.S. Environmental Protection Agency (Grant R82-5377) and the National Science Foundation (Grant BES 93-21274) provided financial support.

References and Notes

(1) Atkinson, R.; Arey, J. *Environ. Health Perspect.* **1994**, *102*, 117−126.
(2) Hites, R. A. *Acc. Chem. Res.* **1990**, *23*, 196−201.
(3) Shroeder, W. H.; Lane, D. A. *Environ. Sci. Technol.* **1988**, *22*, 240−246.
(4) Ballschmiter, K. *Angew. Chem.* **1992**, *31*, 487−664.
(5) Eitzer, B. D.; Hites, R. A. *Environ. Sci. Technol.* **1989**, *23*, 1389−1395.
(6) Hippelein, M.; Kaupp, H.; Dorr, G.; McLachlan, M.; Hutzinger, O. *Chemosphere* **1996**, *32*, 1605−1616.
(7) Atkinson, R. In *Issues in Environmental Science and Technology*; Hester, R. E., Harrison, R. M., Eds.; The Royal Society of Chemistry: Cambridge, UK, 1996; Vol. 6, pp 53−72.
(8) Atkinson, R. *J. Phys. Chem. Ref. Data, Monogr. 1* **1989**, 1−246.
(9) Anderson, P. N.; Hites, R. A. *Environ. Sci. Technol.* **1996**, *30*, 301−306.
(10) Seinfeld, J. H. *Atmospheric Chemistry and Physics of Air Pollution*; Wiley: New York, 1986.
(11) Anderson, P. N.; Hites, R. A. *Environ. Sci. Technol.* **1996**, *30*, 1756−1763.
(12) Kwok, E. S. K.; Arey, J.; Atkinson, R. *Environ. Sci. Technol.* **1994**, *28*, 528−533.
(13) Kwok, E. S. K.; Atkinson, R.; Arey, J. *Environ. Sci. Technol.* **1995**, *29*, 1591−1598.
(14) Brubaker, W. W.; Hites, R. A. *Environ. Sci. Technol.* **1997**, *31*, 1805−1810.
(15) Atkinson, R. *Chem. Rev. (Washington, D.C.)* **1986**, *86*, 69−201.
(16) Atkinson, R. *J. Phys. Chem. Ref. Data, Monogr. 2* **1994**, 1−216.
(17) Finlayson-Pitts, B. J.; Pitts, J. N. *Atmospheric Chemistry: Fundamentals and Experimental Techniques;* Wiley: New York, 1986; pp 883−887.
(18) Kwok, E. S. C.; Atkinson, R. *Atmos. Environ.* **1995**, *29*, 1685−1695.
(19) Lorenz, K.; Zellner, R. *Ber. Bunsen-Ges. Phys. Chem.* **1983**, *87*, 629−636.
(20) (a) Klopffer, W.; Frank, R.; Kohl, E. G.; Haag, F. *Chem.-Ztg.* **1986**, *110*, 57. (b) Methods of the Ecotoxicological Evaluation of Chemicals, Photochemical Degradation in the Gas Phase. In Vol. 6, *OH Reaction Rate Constants and Tropospheric Lifetimes of Selected Environmental Chemicals*; Report 1980−1983; Becker, K. H., Biehl, H. M., Bruckman, P., Fink, E. H., Fuhr, F., Klopffer, W., Zellner, R., Zetzsch, C., Eds.; Kernforschungsanlage: Juelich GmbH, Nov 1984.
(21) Atkinson, R.; Aschmann, S. M. *Int. J. Chem. Kinet.* **1988**, *20*, 513−539.
(22) Klopffer, W.; Haag, F.; Khol, E. G.; Frank, R. *Ecotoxicol. Environ. Saf.* **1988**, *15*, 298−319.
(23) Klamt, A. *Chemosphere* **1993**, *26*, 1273−1289.
(24) Kwok, E. S. C.; Atkinson, R.; Arey, J. *Int. J. Chem. Kinet.* **1997**, *29*, 299−309.
(25) Biermann, H. W.; MacLoed, H.; Atkinson, R.; Winer, A. M.; Pitts, J. N. *Environ. Sci. Technol.* **1985**, *19*, 244−248.
(26) Kwok, E. S. K.; Harger, W. P.; Arey, J.; Atkinson, R. *Environ. Sci. Technol.* **1994**, *28*, 521−527.
(27) Helmig, D.; Arey, J.; Atkinson, R.; Harger, W. P.; McElroy, P. A. *Atmos. Environ.* **1992**, *26A*, 1735−1745.
(28) Helmig, D.; Harger, E. P. *Sci. Total Environ.* **1994**, *148*, 11−21.
(29) Hites, R. A.; Simonsick, W. J. *Calculated Molecular Properties of Polycyclic Aromatic Hydrocarbons*; Elsevier: New York, 1987; pp 21, 24.
(30) Mackay, D.; Shiu, W. Y.; Ma, K. C. *Illustrated Handbook of Physical-Chemical Properties and Environmental Fate for Organic Chemicals*; Lewis Publishers: Ann Arbor, 1992.
(31) Prinn, R. G.; Weiss, R. F.; Miller, B. R.; Huang, J.; Alyea, F. N.; Cunnold, D. M.; Fraser, P. J.; Hartley, H. E.; Simmonds, P. G. *Science* **1995**, *259*, 187−192.